

Circular RNA circGTIC1 drives gastric TIC self-renewal to initiate gastric tumorigenesis and metastasis

Running title: circGTIC1 drives gastric TIC self-renewal

Liyan Wang¹, Bin Li¹#, Xuhua Xiao¹, Xiaoyuan Yi¹, Feifei He¹

¹ Department of Digestive Medicine, Affiliated Hospital of Guilin Medical University.

No. 15 Lequn Road, Xiufeng District, Guilin City, Guangxi Zhuang Autonomous Region.

#Correspondence and requests for materials should be addressed to B Li (email: BinLighy@163.com).

WITHDRAWN
see manuscript DOI for details

Abstract

Gastric cancer is one of the most serious cancers all over the world. Gastric tumor initiating cells (TIC) account for gastric tumorigenesis and metastasis. Here we identified circGTIC1 as a highly expressed circRNA in gastric cancer and gastric TICs. circGTIC1 knockout inhibited the self-renewal of gastric TICs and metastasis, and its overexpression activated gastric TICs. circGTIC1 drove the expression of Sox8 and exerted its role via Sox8-dependent manner. circGTIC1 associated with Ino80 chromatin remodeling complex, and recruited Ino80 complex to Sox8 promoter, finally initiated Sox8 expression. Our work revealed a novel circRNA to regulate gastric tumorigenesis and gastric TICs, adding a new layer for gastric TIC regulation and circRNA functions. CircGTIC1 plays a central role in gastric TIC self-renewal and metastasis. circGTIC1 drives the expression of Sox8 through recruiting Ino80 complex to Sox8 promoter. circGTIC1-Ino80-Sox8 axis can be used for gastric tumor and gastric TIC targeting. Our work revealed a novel circRNA to regulate gastric tumorigenesis and gastric TICs, adding a new layer for gastric TIC regulation and circRNA functions

Keyword: circGTIC1, gastric tumorigenesis, gastric, Ino80 complex, Sox8

Introduction

Gastric cancer is one of the most serious cancers in the world, leading to hundreds of thousands of deaths(R Garcia 2015). There are various cells in gastric tumor bulk, and many tumor cells can't initiate new tumors efficiently(S Takaishi *et al.* 2008). Only a small subset of cells in tumor bulk drive tumor initiation efficiency, which are termed as tumor initiating cells (TICs) or cancer stem cells (CSCs)(E Batlle *et al.* 2017). Gastric TICs harbor self-renewal and differentiation capacities. Recently several surface markers of gastric TICs have been identified, including CD44, ALDH1, CD24, CD133, EPCAM and so on (S Takaishi *et al.* 2009; Y Wakamatsu *et al.* 2012; CJ Zhang *et al.* 2011). Gastric TICs can propagate into oncospheres in FBS-free medium and sphere formation emerges as a standard assay for gastric TIC detection (ME Han *et al.* 2011). Meanwhile, gastric TICs account for tumor metastasis and show enhanced invasion capacity in transwell assay(ME Han *et al.* 2013). Despite of the importance of gastric TICs, their biology remain elusive.

The self-renewal of TICs is finely regulated, and several signaling pathways are involved in TIC regulation, including Wnt/β-catenin, Notch, PKC and Hedgehog pathways(Z Chen *et al.* 2018a; Z Chen *et al.* 2018b; N Takebe *et al.* 2015; P Zhu *et al.* 2015). Gastric TICs are also regulated by several transcription factors, including Gli1, Sox2 and RUNX3. RUNX3 activates gastric TICs through miR-30a/vimentin axis(Z Liu *et al.* 2014). Gli1 plays an essential role in stem-characteristic acquirement of gastric TICs(D Yu *et al.* 2014). Sox2 promotes gastric tumorigenesis and drug resistance of gastric TICs(T Tian *et al.* 2012). Sox8 is another member of Sox transcription factor family. Sox8 plays an oncogenic role in non-small cell lung cancer (C Xie *et al.* 2014), hepatocellular carcinoma (S Zhang *et al.* 2014) and tongue squamous cell carcinoma(SL Xie *et al.* 2018). However, its role in gastric tumorigenesis and gastric TICs is unknown. Here we found Sox8 was highly expressed in gastric cancers and gastric TICs, and drove the self-renewal of gastric TICs.

circRNAs are a type of circular non-coding RNA molecules those are generated by covalently binding between the 5' end and 3' ends after back splicing(LL Chen 2016).

circRNAs are widely distributed in various cells, with structural stability, sequence conservation and tissue specificity(SJ Conn *et al.* 2015; S Memczak *et al.* 2013). circRNAs are derived from precursor RNA molecules by spliceosomes or ribozyme, and several circRNAs may be originated from a single RNA because of variable cyclization(Z Li *et al.* 2015; L Szabo *et al.* 2016; XO Zhang *et al.* 2014; Y Zhang *et al.* 2013). circRNAs were considered as byproducts of RNA splicing, but recently increasing evidences emerge that circRNA are critical modulators in many physiological and pathological processes. Multiple circRNAs function as microRNA sponges(TB Hansen *et al.* 2013; S Memczak *et al.* 2013). Loss of Cdr1as results in miRNA deregulation and neuropsychiatric disorder(M Piwecka *et al.* 2017). circRNAs regulate their parental genes' expression by interaction with U1 snoRNA or Polymerase II (Z Li *et al.* 2015). Generating from chromosomal translocated regions, fusion circRNAs contribute to proliferation, transformation and tumorigenesis(J Guarnerio *et al.* 2016). circFoxo3 are reported to regulated cell cycle progression(WW Du *et al.* 2016). Increasing functional circRNAs are identified. However, the functions of circRNAs in gastric tumorigenesis, metastasis and gastric TIC self-renewal remain unclear. In this study, we identified that circGTIC1 is highly expressed in gastric cancer and gastric TICs. circGTIC1 plays an essential role in the self-renewal of gastric TICs and metastasis. circGTIC1 recruits Ino80 complex for Sox8 expression, which further initiates gastric tumorigenesis, metastasis and TIC self-renewal.

Results

circGTIC1 was highly expressed in gastric TICs

circRNAs are modulators in many biological processes, but their roles in gastric tumorigenesis and gastric TIC self-renewal are unknown. To identify functional circRNAs in gastric tumorigenesis and gastric TICs, we performed a unbiased screening using online available datasets, and found two conserved circRNAs were highly expressed in gastric tumors (Figure 1A). Through sphere formation assay,

has_circ_0045190 (hereafter termed as circGTIC1, abbreviated for circRNA for Gastric Tumor Initiating Cells #1) was selected as its depletion largely impaired the self-renewal of gastric TICs (Figure 2B).

CircGTIC1 is derived from TANC2 precursor RNA and contains two exons (Supplementary Figure 1A). PCR and sequencing confirmed circGTIC1 as a circRNA (Supplementary Figure 1B). CircRNAs show enhanced stability than linear RNA, and thus have much longer half-life time. As expected, circGTIC1 resisted to actinomycin D and RNase R treatment (Supplementary Figure 1C, D).

circGTIC1 was highly expressed in primary gastric tumors, especially in advanced tumors (Figure 1C, D). A gastric tumor tissue array was also performed to examine the expression of circGTIC1. circGTIC1 was highly expressed in serious gastric tumors (Figure 1E, F), and its expression levels were related to clinical prognosis (Figure 1G).

To detect the expression of circGTIC1 in gastric TICs, we enriched TIC through FACS or through sphere formation assay. We found circGTIC1 was highly expressed in TICs and oncospheres (Figure 1H, I). The high expression of circGTIC1 was confirmed by Northern blot (Figure 1J) and FISH (Figure 1K). Altogether, circGTIC1 was highly expressed in gastric cancer and gastric TICs.

circGTIC1 knockout attenuated gastric TIC self-renewal and metastasis

To evaluate the role of circGTIC1 in gastric TICs, we generated *circGTIC1* knockout cells. We identified two intron sequences were necessary for the generation of circGTIC1 (Supplementary Figure 1E, F), and generated *circGTIC1* knockout through CRISPR/Cas9 approach (Supplementary Figure 1G). Two *circGTIC1* knockout cells were generated and confirmed by PCR, sequencing and circGTIC1 expression detection (Figure 2A and Supplementary Figure 1H). We found *circGTIC1* deficiency didn't influence the expression of TANC2 mRNA, nor cell apoptosis, but inhibited the stemness, proliferation and metastasis (Figure 2B). Decreased TIC ratios were examined upon *circGTIC1* knockout, indicating the critical role of circGTIC1 in gastric TIC maintenance (Figure 2C). We also examined the self-renewal of gastric TICs through sphere formation assay, and found *circGTIC1* knockout generated

decreased spheres, indicating the critical role of circGTIC1 in gastric TIC self-renewal (Figure 2D). We also examined the proliferation of *circGTIC1* knockout spheres. We stained proliferating cells with Ki67 and CFSE assay, and found *circGTIC1* knockout inhibited the propagation of gastric TICs (Figure 2E, F). Moreover, gradient dilution tumor initiation assay also confirmed the essential role of circGTIC1 in gastric tumor initiation (Figure 2G). Decreased TIC ratios were also detected upon *circGTIC1* knockout (Figure 2H). Considering the critical role of gastric TICs in tumor invasion and metastasis, we detected tumor invasion through transwell assay, and found impaired invasion of *circGTIC1* knockout cells (Figure 2I). To further detect the role of circGTIC1 in gastric tumor propagation, we established tumor propagation assay with *circGTIC1* knockout cells. As expected, *circGTIC1* knockout inhibited tumor propagation (Figure 2J). We also challenged the role of circGTIC1 using established tumors. We generated 400 mm³ tumors and treated with circGTIC1 ASO and traditional drug 5-FU, and found 5-FU treatment alone induced tumor relapse. While, combination of 5-FU and ASO drove sustained tumor elimination (Figure 2K). Impaired stemness, propagation, metastasis, and enhanced apoptosis were observed upon combined treatment (Figure 2L). Taken together, circGTIC1 drove gastric TIC self-renewal and metastasis.

***circGTIC1* overexpression promoted gastric TIC self-renewal**

To further examine the role of circGTIC1, we generated circGTIC1 overexpression cells (Figure 3A). circGTIC1 overexpression led to increased TIC ratios (Figure 3B) and enhanced self-renewal (Figure 3C). Ki67 staining and CFSE assay confirmed the increase of proliferating TICs (Figure 3D, E). Tumor initiation assay also validated the critical role of circGTIC1 in gastric tumor initiation (Figure 3F). Similarly, increased TIC ratios were measured upon circGTIC1 overexpression (Figure 3G). circGTIC1 overexpression also drove tumor propagation (Figure 3H) and metastasis (Figure 3I).

To further confirm the correlation between circGTIC1 and gastric TIC characteristics, we collected primary samples and divided them into two groups according to circGTIC1 expression, and examined the expression of TIC marker, propagation and

metastasis associated proteins. As shown in Figure 3J, circGTIC1^{high} samples showed enhanced expression of TIC marker, proliferation and metastasis proteins, further confirming the role of circGTIC1 in tumor TICs, propagation and metastasis. We also examined sphere formation and metastasis of circGTIC1^{high} and circGTIC1^{low} samples, and found circGTIC1 was positively related to gastric TIC self-renewal and invasion (Figure 3K, L)

We overexpressed mouse circGTIC1 (termed as circGtic1) in mice, and induced gastric tumors through Helicobacterpylori/MNNG method (Supplementary Figure 1I). circGTIC1 overexpression promoted tumor formation and increased tumor volume (Figure 3M). Altogether, circGTIC1 drove gastric tumorigenesis, TIC self-renewal and metastasis.

circGTIC1 drove Sox8 expression

To identify the target genes of circGTIC1, we performed RNA-seq assay using *circGTIC1* knockout cells and found Sox8 was the lowest expressed upon *circGTIC1* knockout (Figure 4A). Western blot confirmed the impairment of Sox8 expression in *circGTIC1* knockout cells (Figure 4B). On the contrary, circGTIC1 overexpressing cells showed an enhanced Sox8 expression (Figure 4C). We examined Sox8 expression and found a positive correlation between circGTIC1 and Sox8 (Figure 4D), which was confirmed by Northern blot (Figure 4E).

We then generated *Sox8* knockout cells through CRISPR/Cas9 approach, and confirmed knockout efficiency with Western blot (Figure 4F). We silenced circGTIC1 expression in *Sox8* knockout cells, and found comparable self-renewal and metastasis, indicating the critical role of Sox8 in circGTIC1 function (Figure 4G, H). Similarly, circGTIC1 overexpression also showed impaired role in gastric TIC self-renewal and metastasis upon *Sox8* knockout (Figure 4I, J). Taken together, circGTIC1 promoted gastric TIC self-renewal and metastasis through Sox8-dependent manner.

circGTIC1 interacted with Ino80 complex

To further explore the molecular mechanism of circGTIC1, we performed RAP (RNA antisense purification) assay and identified the specific band in circGTIC1 samples as Ino80 by mass spectrum (Figure 5A). Ino80 was the core component of Ino80

complex, which contain Ino80, Ruvbl1 and Ruvbl2 (JY Jin *et al.* 2005). We confirmed the interaction between circGTIC1 and Ino80 complex through Western blot (Figure 5B). RIP (RNA immunoprecipitation) also confirmed the binding of circGTIC1 and Ino80 in gastric TICs (Figure 5C). The direct binding of circGTIC1 and Ino80 was validated by EMSA (Figure 5D). Finally, we stained circGTIC1 and Ino80 in spheres, and also confirmed their co-localization (Figure 5E).

We then examined the expression pattern of Ino80 complex. Interestingly, three components of Ino80 complex (Ino80, Ruvbl1 and Ruvbl2) were all highly expressed in gastric tumors and related to clinical severity (Figure 5F). Moreover, Ino80 complex was also highly expressed in gastric TICs (Figure 5G, H). Altogether, circGTIC1 combined with Ino80 complex that was highly expressed in gastric tumors and TICs.

circGTIC1 recruited Ino80 complex to Sox8 promoter

We then explored the molecular mechanisms of Ino80 complex and circGTIC1 in Sox8 expression. Both Ino80 and circGTIC1 bind to the same region of *Sox8* promoter (Figure 6A, B). Interestingly, impaired binding of Ino80 to *Sox8* promoter was observed upon *circGTIC1* knockout (Figure 6C). On the contrary, circGTIC1 overexpression led to an enhanced combination of Ino80 complex and *Sox8* promoter (Figure 6D). These observation indicated the essential role of circGTIC1 in Ino80-*Sox8* promoter combination. We also observed the subcellular location of Ino80 and *Sox8* promoter, and confirmed their co-localization in WT cells. However, impaired co-localization of Ino80 and *Sox8* promoter was observed upon *circGTIC1* knockout, further indicating the critical role of circGTIC1 in Ino80-*Sox8* promoter interaction (Figure 6E). Ino80 components and *Sox8* promoter were in same fractions of Ino80 ChIP eluate, but in *circGTIC1* knockout cells, impaired enrichment of *Sox8* promoter was observed (Figure 6F). In conclusion, circGTIC1 recruited Ino80 complex to *Sox8* promoter.

We then generated *Ino80* knockout cells, and found impaired expression of *Sox8*, indicating the critical role of Ino80 complex in *Sox8* expression (Figure 6G). *circGTIC1* knockout or *Ino80* knockout inhibited the activation of *Sox8* promoter, and

circGTIC1 overexpression promoted the activation of *Sox8* promoter (Figure 6H, I). As a major hallmark for transcriptional activation, H3K4me3 was also impaired in *circGTIC1* knockout and *Ino80* knockout cells, and was increased upon circGTIC1 overexpression (Figure 6J, K). RNA polymerase II ChIP assay also confirmed the critical role of circGTIC1 and Ino80 in *Sox8* transcriptional activation (Figure 6L, M). To further examine the role of Ino80 complex in circGTIC1 function, we overexpressed circGTIC1 in *Ino80* knockout cells, and found circGTIC1 overexpression had impaired role in *Sox8* expression upon *Ino80* knockout, indicating the essential role of Ino80 in circGTIC1 function (Figure 6N). We also generated *Sox8* promoter knockout cells through deleting the Ino80-circGTIC1 binding region of *Sox8* promoter (Supplementary Figure 1J). *Sox8* promoter knockout impaired the expression of *Sox8*. Moreover, circGTIC1 overexpression had an impaired role in *Sox8* expression upon *Sox8* promoter knockout, indicating an essential role of circGTIC1-*Sox8* promoter interaction in circGTIC1 function (Figure 6N). Consistent with *Sox8* expression, circGTIC1 overexpression showed impaired influence on sphere formation and metastasis upon *Ino80* knockout or *Sox8* promoter knockout (Figure 6O, P). Taken together, circGTIC1 recruited Ino80 complex to *Sox8* promoter, and drove *Sox8* expression, gastric TIC self-renewal and metastasis by binding to *Sox8* promoter.

Sox8 was a core modulator for gastric TICs

Sox8 plays an oncogenic role in several cancers, but its role in gastric tumorigenesis is unclear. Here, we examined the role of *Sox8* in gastric tumorigenesis and gastric TIC self-renewal. *Sox8* was highly expressed in gastric tumors, especially in advanced gastric tumors (Figure 7A, B). Gastric tumor tissue array also revealed an increased expression of *Sox8* in gastric tumors (Figure 7C). *Sox8* expression was also related to clinical prognosis (Figure 7D). We also examined *Sox8* expression in gastric TICs and found *Sox8* was highly expressed in gastric TICs (Figure 7E).

Sox8 knockout cells showed decreased TIC ratios, and impaired self-renewal capacity (Figure 7F, G). Decreased proliferation in gastric TICs were also detected upon *Sox8* deletion (Figure 7H). *Sox8* knockout also inhibited tumor invasion (Figure 7I). These

results revealed the essential role of Sox8 in gastric TIC self-renewal and metastasis.

We then restored Sox8 expression in *circGTIC1* knockout cells (Figure 7J). Sox8 overexpression restored the impaired self-renewal and metastasis induced by *circGTIC1* knockout, confirming that *circGTIC1* promote gastric TIC self-renewal and metastasis through Sox8 (Figure 7K, L). Altogether, Sox8 drove the self-renewal of gastric TICs and served as a functional target gene of *circGTIC1*.

Discussion

Gastric tumor initiating cells account for gastric tumorigenesis and metastasis, but their regulation are poorly understood. Here we screened circRNAs using online available datasets, and identified *circGTIC1* was highly expressed in gastric cancer and gastric TICs. Through loss of function assay, sphere formation assay, transwell invasion assay, tumor propagation assay and tumor initiating assay, we proved *circGTIC1* as a critical modulator for gastric TICs. Our work revealed a novel circRNA in gastric tumorigenesis and added a new layer for gastric TIC regulation.

As we know, gene knockout emerges as a critical strategy to investigate the function of biological molecules(L Rossi *et al.* 2012). However, rare circRNA knockout assays have been reported. The generation of circRNA is elusive, and difficult to be disrupted. Moreover, many circRNAs are originated from precursor RNA, and their knockout probably disturbs the expression of the corresponding linear RNAs(A Ivanov *et al.* 2015). Piwecka et al found *Cdr1as* locus only generated circRNA but no corresponding linear RNA, thus generated a *Cdr1as* knockout mice through deleting the total region of *Cdr1as* locus(M Piwecka *et al.* 2017). Many circRNAs are generated from covalently binding between the 5' end and 3' ends after back splicing, and the reverse complementary sequences flanking of circRNAs were necessary for the generation of many circRNAs(SP Barrett *et al.* 2015). Taking advantage of this characteristic, Xia et al developed a strategy to delete circRNA (PY Xia *et al.* 2018). Here we generated *circGTIC1* knockout cells through similar strategy. Using *circGTIC1* knockout cells, we validated the role of *circGTIC1*, adding a novel role of circRNAs and a new layer for TIC regulation.

As we know, metastasis is a major cause for tumor-induced cell death(L Seguin *et al.* 2015). The critical role of TICs in tumor metastasis was well-known for long time(Z Chen *et al.* 2018c; F Li *et al.* 2007). TICs harbor enhanced metastasis capacity, and increasing evidences prove that invasive cells contain many TIC characteristics (A Kreso *et al.* 2014). In this work, we found circGTIC1 was not only required for the self-renewal of gastric TICs, but also promoted tumor invasion. Our finding confirmed the critical role of TICs in tumor invasion and metastasis.

As critical regulators for tumorigenesis, metastasis and drug resistance, TICs emerge as promising targets for tumor elimination. Gastric TICs are also optimal targets for gastric tumor targeting(SR Singh 2013). However, TICs are resistant to traditional drugs, with high expression of pump molecules like ABCG2(ZZ Chen *et al.* 2016). Moreover, several evidences indicated that targeting TICs only leads to a transdifferentiation from non-TICs to TICs, resulting in a failure of TIC-targeting therapy(MC Cabrera *et al.* 2015; PP Zhu *et al.* 2017). Thus, combination of TIC-targeting and traditional therapy is a promising strategy for tumor targeting. In this work, we found traditional drug 5-FU led to tumor elimination in the beginning, but increased tumor volume was observed soon. If we combined 5-FU with TIC-targeting ASO together, the tumors were eliminated continuously. Moreover, upon 5-FU treatment, TIC surface marker CD44 was increased, indicating a enrichment of gastric TICs after drug treatment. The increment of gastric TICs may account for tumor relapse and metastasis. Only treated with 5-FU and ASO together, gastric TICs were decreased and tumor volume was decreased. Our finding confirmed the necessary to combine gastric TIC therapy and traditional therapy together.

Chromatin remodeling complexes play critical roles in many processes, including transcription initiation(CR Clapier *et al.* 2009). It's a common sense that chromatin remodeling complexes are conserved in many species and their expression levels are unlikely to change a lot. However, we found Ino80 chromatin remodeling complex was highly expressed in gastric cancers and gastric TICs. Actually, several chromatin remodeling complexes are deregulated in tumorigenesis. NURF, PRC2 and BRG1 were highly expressed in liver cancer and liver TICs, while, BRM typed SWI/SNF

complex was lowly expressed in liver cancer and liver TICs(PP Zhu *et al.* 2015; PP Zhu *et al.* 2016a; PP Zhu *et al.* 2016b). Here we revealed a high expression of Ino80 in gastric cancer and gastric TICs. Moreover, Ino80 was required for the self-renewal of gastric TICs, serving as a potential target for gastric tumorigenesis and gastric TICs. The clinical application of Ino80 complex needs to be further investigated.

CircRNAs exert their roles through various mechanisms (J Salzman 2016). Here we found circGTIC1 drove the self-renewal of gastric TICs through Sox8 through recruiting Ino80 complex to *Sox8* promoter. Like other biological molecules, circGTIC1 changes the expression of many genes, and here we identified Sox8 was the functional target gene of circGTIC1 in gastric TIC self-renewal. We established *Sox8* knockout cells and then overexpressed circGTIC1, and found impaired role of circGTIC1 upon *Sox8* knockout, indicating the critical role of Sox8 in circGTIC1 function. We also rescued *Sox8* expression in *circGTIC1* knockout cells, and found a restored self-renewal and metastasis. These findings indicated that circGTIC1 drove gastric TIC self-renewal and metastasis through *Sox8*-dependent manner.

Methods

Reagents and materials

Anti-CD44 (Cat. No. 15675-1-AP), anti-β-actin (Cat. No. 66009-1-Ig), anti-PCNA (Cat. No. 10205-2-AP), anti-*Sox8* (Cat.No 20627-1-AP), anti-Ruvbl1 (Cat.No 10210-2-AP), anti-Ruvbl2 (Cat.No 10195-1-AP) and anti-CCND1 (Cat.No 60186-1-Ig) antibodies were purchased from Proteintech Company. Anti-BID (Cat. No. 2002), anti-BAX (Cat. No. 5023), anti-Mmp2 (Cat.No 40994), anti-Mmp7 (Cat.No 3801) and anti-Ki67 (Cat.No 9449) antibodies were from Cell Signaling Technology; anti-Ino80 (Cat.No ab105451) and anti-TANC2 (Cat. No. ab121745) antibodies were from Abcam company. N2 and B27 supplements were obtained from Invitrogen; EGF and FGF were purchased from PeproTech. DAPI (4',6-diamidino-2-phenylindole) was purchased from Sigma-Aldrich. All the primers were generated from Sangon Company and the sequences were shown in Supplementary Table 1.

circGTIC1 knockout

circGTIC1 knockout cells were generated as described (34). Two sequences flanking of *circGTIC1* were detected by minigene assay, and deleted by CRISPR/Cas9 approach. For monoclonalization, Cas9 lentivirus infected cells were seeded into 96-well plate (one cell per well), and cultured in sphere formation medium for single colon formation. The expression of *circGTIC1* in generated colons were examined by realtime PCR and the knockout was confirmed by sequencing. Two knockout strategies were used for *circGTIC1* knockout, one deleting the left complementary sequence and the other deleting the right (Supplementary Figure 1E-H).

Gastric TIC enrichment and detection

$CD44^+ EPCAM^+$ gastric TICs in gastric tumor bulk were enriched or detected. For TIC enrichment, primary samples were digested into single cells, and stained with CD44 and EPCAM antibodies. $CD44^+ EPCAM^+$ cells were enriched by FACS. For TIC detection, *circGTIC1* knockout, *circGTIC1* overexpression and control cells were used for FACS detection, the ratios of $CD44^+ EPCAM^+$ cells were considered as TIC ratios.

Sphere formation

Sphere formation assay was performed as described(5). Briefly, gastric TICs were incubated in Neurobasal-A medium (supplemented with 2 mM l-glutamine, B27, N2, 50 ng/ml of EGF, 50 ng/ml of FGF). Two weeks later, spheres formation ratios were calculated and spheres were collected for further experiments.

Tumor propagation and tumor initiation assay

For tumor propagation assay, 1×10^6 *circGTIC1* knockout, *circGTIC1* overexpression and control cells were subcutaneously injected into BALB/c nude mice. Tumor volumes were measured every three days. For tumor initiation assay, 10, 1×10^2 , 1×10^3 , 1×10^4 , and 1×10^5 cells were subcutaneously injected into BALB/c nude mice. Three month later, tumor formation was observed and TIC ratios were calculated through extreme limiting dilution analysis (<http://bioinf.wehi.edu.au/software/elda/>) (48).

Transwell invasion assay

For invasion assay, transwells were coated with Matrigel. *circGTIC1* knockout, *circGTIC1* overexpressed or control TICs were cultured in FBS-free medium and

seeded in wells. FBS-supplemented medium was used outside. 36 hours later, cells didn't pass through Matrigel were removed and the passed cells were stained with crystal violet for observation.

Western blot

For Western blot, the indicated samples were subjected into SDS-PAGE for protein-separation, and samples were then transferred onto nitrocellulose membrane. Then the samples were incubated with the indicated primary antibodies, followed by HRP-conjugated secondary antibodies for visualization.

Immunohistochemistry

For immunohistochemistry, 5- μ m sections were produced from paraffin-coated samples, treated with xylol and ethanol, followed by treatment with 3% H₂O₂. The samples were boiled for 15min in Tris-EDTA buffer for antigen retrieval, then incubated with primary antibodies for 2 hours, followed by 1 hour's HRP-conjugated secondary antibody. Finally the sections were treated with DAB substrate for visualization.

Statistics

For each assay, at least three individual experiments were repeated and typical results were shown. Two tailed T-test was examined for most assays. P<0.05 was considered as statistical significant. *, P<0.05; **, P<0.01; ***, P<0.001.

Ethics approval and consent to participate

Primary gastric tumor samples were from Department of Digestive Medicine, Affiliated Hospital of Guilin Medical University, with informed consent.

Acknowledgement

None.

Consent for publication

The author agree for publication.

Availability of data and material

All data and materials can be provided upon request.

Competing financial interests:

The authors declare no competing financial interest after they read the final version of

the manuscript

Funding

This work was supported by Special fund for the development of science and technology (81560402).

Author contributions

Wang. L. performed experiments, analyzed data and wrote the paper; Xiao, X., Yi, X., and He, F. performed some experiments; Li, B. initiated the study, designed experiments and wrote the paper.

References

- Barrett SP ,Wang PL ,Salzman J (2015) Circular RNA biogenesis can proceed through an exon-containing lariat precursor. *Elife* **4**: e07000
- Batlle E,Clevers H (2017) Cancer stem cells revisited. *Nature medicine* **23(10)**: 1124-1134
- Cabrera MC ,Hollingsworth RE ,Hurt EM (2015) Cancer stem cell plasticity and tumor hierarchy. *World J Stem Cells* **7(1)**: 27-36
- Chen LL (2016) The biogenesis and emerging roles of circular RNAs. *Nature reviews. Molecular cell biology* **17(4)**: 205-211
- Chen Z ,Gao Y ,Yao L ,Liu Y ,Huang L ,Yan Z ,Zhao W ,Zhu P ,Weng H (2018a) LncFZD6 initiates Wnt/beta-catenin and liver TIC self-renewal through BRG1-mediated FZD6 transcriptional activation. *Oncogene* **37(23)**: 3098-3112
- Chen Z ,Liu Y ,Yao L ,Guo S ,Gao Y ,Zhu P (2018b) The long noncoding RNA IncZic2 drives the self-renewal of liver tumor-initiating cells via the protein kinase C substrates MARCKS and MARCKSL1. *The Journal of biological chemistry* **293(21)**: 7982-7992
- Chen Z ,Yao L ,Liu Y ,Zhu P (2018c) LncTIC1 interacts with beta-catenin to drive liver TIC self-renewal and liver tumorigenesis. *Cancer Lett* **430**:88-96
- Chen ZZ ,Zhu PP ,Zhang YS ,Liu YT ,He YL ,Zhang LF ,Gao YF (2016) Enhanced Sensitivity of Cancer Stem Cells to Chemotherapy Using Functionalized Mesoporous Silica Nanoparticles. *Mol Pharmaceut* **13(8)**: 2749-2759
- Clapier CR ,Cairns BR (2009) The Biology of Chromatin Remodeling Complexes. *Annu Rev Biochem* **78**(273-304)
- Conn SJ ,Pillman KA ,Toubia J ,Conn VM ,Salmanidis M ,Phillips CA ,Roslan S ,Schreiber AW ,Gregory PA ,Goodall GJ (2015) The RNA binding protein quaking regulates formation of circRNAs. *Cell* **160(6)**: 1125-1134
- Du WW ,Yang W ,Liu E ,Yang Z ,Dhaliwal P ,Yang BB (2016) Foxo3 circular RNA retards cell cycle progression via forming ternary complexes with p21 and CDK2. *Nucleic acids research* **44(6)**: 2846-2858
- Garcia R (2015) Epidemiology and characteristics of gastric cancer in national cancer institute of Panama from the years 2007 to 2011. *J Clin Oncol* **33(15)**:

- Guarnerio J ,Bezzi M ,Jeong JC ,Paffenholz SV ,Berry K ,Naldini MM ,Lo-Coco F ,Tay Y ,Beck AH ,Pandolfi PP (2016) Oncogenic Role of Fusion-circRNAs Derived from Cancer-Associated Chromosomal Translocations. *Cell* **165**(2): 289-302
- Han ME ,Jeon TY ,Hwang SH ,Lee YS ,Kim HJ ,Shim HE ,Yoon S ,Baek SY ,Kim BS ,Kang CD ,Oh SO (2011) Cancer spheres from gastric cancer patients provide an ideal model system for cancer stem cell research. *Cell Mol Life Sci* **68**(21): 3589-3605
- Han ME ,Oh SO (2013) Gastric stem cells and gastric cancer stem cells. *Anatomy & cell biology* **46**(1): 8-18
- Hansen TB ,Jensen TI ,Clausen BH ,Bramsen JB ,Finsen B ,Damgaard CK ,Kjems J (2013) Natural RNA circles function as efficient microRNA sponges. *Nature* **495**(7441): 384-388
- Ivanov A ,Memczak S ,Wyler E ,Torti F ,Porath HT ,Orejuela MR ,Piechotta M ,Levanon EY ,Landthaler M ,Dieterich C ,Rajewsky N (2015) Analysis of Intron Sequences Reveals Hallmarks of Circular RNA Biogenesis in Animals. *Cell Rep* **10**(2): 170-177
- Jin JY ,Cai Y ,Yao T ,Gottschalk AJ ,Florens L ,Swanson SK ,Gutierrez JL ,Coleman MK ,Workman JL ,Mushegian A ,Washburn MP ,Conaway RC ,Conaway JW (2005) A mammalian chromatin remodeling complex with similarities to the yeast INO80 complex. *Journal of Biological Chemistry* **280**(50): 41207-41212
- Kreso A ,Dick JE (2014) Evolution of the Cancer Stem Cell Model. *Cell Stem Cell* **14**(3): 275-291
- Li F ,Tiede B ,Massague J ,Kang YB (2007) Beyond tumorigenesis: cancer stem cells in metastasis. *Cell Res* **17**(1): 3-14
- Li Z ,Huang C ,Bao C ,Chen L ,Lin M ,Wang X ,Zhong G ,Yu B ,Hu W ,Dai L ,Zhu P ,Chang Z ,Wu Q ,Zhao Y ,Jia Y ,Xu P ,Liu H ,Shan G (2015) Exon-intron circular RNAs regulate transcription in the nucleus. *Nature structural & molecular biology* **22**(3): 256-264
- Liu Z ,Chen L ,Zhang X ,Xu X ,Xing H ,Zhang Y ,Li W ,Yu H ,Zeng J ,Jia J (2014) RUNX3 regulates vimentin expression via miR-30a during epithelial-mesenchymal transition in gastric cancer cells. *Journal of cellular and molecular medicine* **18**(4): 610-623
- Memczak S ,Jens M ,Elefsinioti A ,Torti F ,Krueger J ,Rybak A ,Maier L ,Mackowiak SD ,Gregersen LH ,Munschauer M ,Loewer A ,Ziebold U ,Landthaler M ,Kocks C ,le Noble F ,Rajewsky N (2013) Circular RNAs are a large class of animal RNAs with regulatory potency. *Nature* **495**(7441): 333-338
- Piwecka M ,Glazar P ,Hernandez-Miranda LR ,Memczak S ,Wolf SA ,Rybak-Wolf A ,Filipchik A ,Klironomos F ,Jara CAC ,Fenske P ,Trimbuch T ,Zywitzka V ,Plass M ,Schreyer L ,Ayoub S ,Kocks C ,Kuhn R ,Rosenmund C ,Birchmeier C ,Rajewsky N (2017) Loss of a mammalian circular RNA locus causes miRNA deregulation and affects brain function. *Science* **357**(6357):
- Rossi L ,Lin KYK ,Boles NC ,Yang LB ,King KY ,Jeong M ,Mayle A ,Goodell MA (2012) Less Is More: Unveiling the Functional Core of Hematopoietic Stem Cells through Knockout Mice. *Cell Stem Cell* **11**(3): 302-317
- Salzman J (2016) Circular RNA Expression: Its Potential Regulation and Function. *Trends in genetics : TIG* **32**(5): 309-316
- Seguin L ,Desgroiselle JS ,Weis SM ,Cheresh DA (2015) Integrins and cancer: regulators of cancer stemness, metastasis, and drug resistance. *Trends Cell Biol* **25**(4): 234-240
- Singh SR (2013) Gastric cancer stem cells: A novel therapeutic target. *Cancer Lett* **338**(1): 110-119
- Szabo L ,Salzman J (2016) Detecting circular RNAs: bioinformatic and experimental challenges. *Nature*

- reviews. Genetics* **17(11)**: 679-692
Takaishi S ,Okumura T ,Wang TC (2008) Gastric cancer stem cells. *J Clin Oncol* **26(17)**: 2876-2882
Takaishi S ,Okumura T ,Tu SP ,Wang SSW ,Shibata W ,Vigneshwaran R ,Gordon SAK ,Shimada Y ,Wang TC (2009) Identification of Gastric Cancer Stem Cells Using the Cell Surface Marker CD44. *Stem Cells* **27(5)**: 1006-1020
Takebe N ,Miele L ,Harris PJ ,Jeong W ,Bando H ,Kahn M ,Yang SX ,Ivy SP (2015) Targeting Notch, Hedgehog, and Wnt pathways in cancer stem cells: clinical update. *Nature reviews. Clinical oncology* **12(8)**: 445-464
Tian T ,Zhang Y ,Wang S ,Zhou J ,Xu S (2012) Sox2 enhances the tumorigenicity and chemoresistance of cancer stem-like cells derived from gastric cancer. *Journal of biomedical research* **26(5)**: 336-345
Wakamatsu Y ,Sakamoto N ,Oo HZ ,Naito Y ,Uraoka N ,Anami K ,Sentani K ,Oue N ,Yasui W (2012) Expression of cancer stem cell markers ALDH1, CD44 and CD133 in primary tumor and lymph node metastasis of gastric cancer. *Pathol Int* **62(2)**: 112-119
Xia PY ,Wang S ,Ye BQ ,Du Y ,Li C ,Xiong Z ,Qu Y ,Fan ZS (2018) A Circular RNA Protects Dormant Hematopoietic Stem Cells from DNA Sensor cGAS-Mediated Exhaustion. *Immunity* **48(4)**: 688-+
Xie C ,Han Y ,Liu Y ,Han L ,Liu J (2014) miRNA-124 down-regulates SOX8 expression and suppresses cell proliferation in non-small cell lung cancer. *International journal of clinical and experimental pathology* **7(10)**: 6534-6542
Xie SL ,Fan S ,Zhang SY ,Chen WX ,Li QX ,Pan GK ,Zhang HQ ,Wang WW ,Weng B ,Zhang Z ,Li JS ,Lin ZY (2018) SOX8 regulates cancer stem-like properties and cisplatin-induced EMT in tongue squamous cell carcinoma by acting on the Wnt/beta-catenin pathway. *International journal of cancer* **142(6)**: 1252-1265
Yu D ,Shin HS ,Lee YS ,Lee D ,Kim S ,Lee YC (2014) Genistein attenuates cancer stem cell characteristics in gastric cancer through the downregulation of Gli1. *Oncology reports* **31(2)**: 673-678
Zhang CJ ,Li CW ,He FT ,Cai YJ ,Yang H (2011) Identification of CD44+CD24+gastric cancer stem cells. *J Cancer Res Clin* **137(11)**: 1679-1686
Zhang S ,Zhu C ,Zhu L ,Liu H ,Liu S ,Zhao N ,Wu J ,Huang X ,Zhang Y ,Jin J ,Ji T ,Ding X (2014) Oncogenicity of the transcription factor SOX8 in hepatocellular carcinoma. *Medical oncology* **31(4)**: 918
Zhang XO ,Wang HB ,Zhang Y ,Lu X ,Chen LL ,Yang L (2014) Complementary sequence-mediated exon circularization. *Cell* **159(1)**: 134-147
Zhang Y ,Zhang XO ,Chen T ,Xiang JF ,Yin QF ,Xing YH ,Zhu S ,Yang L ,Chen LL (2013) Circular intronic long noncoding RNAs. *Molecular cell* **51(6)**: 792-806
Zhu P ,Wang Y ,Du Y ,He L ,Huang G ,Zhang G ,Yan X ,Fan Z (2015) C8orf4 negatively regulates self-renewal of liver cancer stem cells via suppression of NOTCH2 signalling. *Nature communications* **6(7122)**
Zhu PP ,Wang YY ,He L ,Huang GL ,Du Y ,Zhang G ,Yan XL ,Xia PY ,Ye BQ ,Wang S ,Hao L ,Wu JY ,Fan ZS (2015) ZIC2-dependent OCT4 activation drives self-renewal of human liver cancer stem cells. *J Clin Invest* **125(10)**: 3795-3808
Zhu PP ,Wang YY ,Huang GL ,Ye BQ ,Liu BY ,Wu JY ,Du Y ,He L ,Fan ZS (2016a) Inc-beta-Catm elicits EZH2-dependent beta-catenin stabilization and sustains liver CSC self-renewal. *Nature structural & molecular biology* **23(7)**: 631-639

Zhu PP ,Wang YY ,Wu JY ,Huang GL ,Liu BY ,Ye BQ ,Du Y ,Gao GX ,Tian Y ,He L ,Fan ZS (2016b) LncBRM initiates YAP1 signalling activation to drive self-renewal of liver cancer stem cells. *Nature communications* 7(1)

Zhu PP ,Fan ZS (2017) Cancer Stem Cell Niches and Targeted Interventions. *Prog Biochem Biophys* 44(8): 697-708

WITHDRAWN
see manuscript DOI for details

Figure legends

Figure 1. High expression of circGTIC1 in gastric tumor and gastric TICs. (A)

Differently expressed circRNAs in Zhang's cohort (GSE83521) and Wang's cohort (GSE100170) were shown as heatmap. Two conserved circRNAs were found to be highly expressed in both cohorts. (B) circRNA knockdown cells were generated with shRNA lentivirus, followed by sphere formation. Typical images were shown in left panel and sphere formation ratios were in right panel. (C) Realtime PCR analyses for circGTIC1 expression. 20 early gastric tumors (eGC), 30 advanced gastric tumor (aGC) and 50 peri-tumor samples were used for detection. (D) circGTIC1 *in situ* hybridization were performed in 10 eGC, 20 aGC and 30 peri-tumor samples. Typical images and circGTIC1 photon intensities were shown. Scale bars, 50 μ m. (E, F) circGTIC1 *in situ* hybridization was performed with gastric tumor tissue array, which contains 84 peri-tumor, 35 stage I tumors, 51 stage II tumors and 12 stage III tumors. Typical images were shown in E and circGTIC1 photon intensities were shown in F. Scale bars, 50 μ m. (G) 98 gastric samples were divided into two groups according to circGTIC1 expression, followed by Kaplan-Meier survival analysis. (H, I) Realtime PCR analyses for circGTIC1 expression in gastric TICs and gastric oncospheres. For H, gastric TICs and non-TICs were enriched with FACS. For I, spheres were enriched from sphere formation assay. (J) Gastric TICs ($CD44^+ EPCAM^+$) and non-TICs were collected for circGTIC1 detection with Northern blot. CD44 were detected for TIC confirmation. (K) Gastric oncospheres and non-spheres were used for circGTIC1 FISH, and counterstained with CD44 and DAPI, followed by observation under microscope. Scale bars, 10 μ m.

Figure 2. circGTIC1 knockout impaired the self-renewal of gastric TICs. (A)

circGTIC1 knockout cells were generated and knockout efficiency was confirmed by realtime PCR. (B) The expression of indicated proteins in circGTIC1 knockout cells was examined by Western blot. circGTIC1 knockout was confirmed by Northern blot. (C) Gastric TIC ratios in circGTIC1 knockout cells were detected by FACS, and shown as mean \pm s.d. (D) circGTIC1 knockout cells were used for sphere formation. Two weeks later, sphere images were taken and sphere formation ratios were

calculated. (E, F) Proliferation of *circGTIC1* knockout cells was examined by Ki67 staining (E) or CFSE assay (F). (G, H) Gradient gastric tumor cells were injected into BALB/c nude mice, and tumor formation was observed three month later. Tumor formation ratios were shown in G and TIC ratios were calculated through ELDA (<http://bioinf.wehi.edu.au/software/elda/>) and shown in H. CI, confidence interval. (I) *circGTIC1* knockout cells and control cells were used for transwell invasion assay. Typical images and counted cell numbers were shown. (J) 1×10^6 *circGTIC1* knockout or control cells were subcutaneously injected into BALB/c nude mice, and tumor volumes were detected every three days. (K) Gastric tumor cells were injected into BALB/c nude mice for tumor formation. When tumors were about 400 mm^3 , the established gastric tumors were treated with *circGTIC1* ASO or 5-FU, and tumor volume were measured every three days. (L) Nine days (day 9) or 21 days (day 21) post treatment, tumors were obtained for Western blot. The indicated proteins were detected, with β -actin as a loading control. CV, Ctrl ASO+Vehicle; AV, *circGTIC1* ASO+Vechicle; CF, Ctrl ASO+5-FU; AF, *circGTIC1* ASO+Vechicle. CV*, for CV, Day 12 tumors were used.

Figure 3. *circGTIC1* overexpression promoted gastric TIC self-renewal. (A) *circGTIC1* overexpressing cells were generated and confirmed by realtime PCR. oecircGTIC1, overexpressing circGTIC1. (B) Gastric TIC ratios were detected by FACS in *circGTIC1* overexpressing cells. (C) *circGTIC1* overexpressing cells and control cells were used for sphere formation assay. Two weeks later, spheres images and sphere formation ratios were observed. Scale bars, $500 \mu\text{m}$. (D, E) Proliferation of *circGTIC1* overexpressing cells was examined by Ki67 staining and CFSE assay. Oecirc, overexpressing circGTIC1. Scale bars, $50 \mu\text{m}$. (F, G) Gradient tumor cells were injected into BALB/c nude mice, and tumor formation was observed three month later. The ratios of tumor formation mice were shown in F, and TIC ratios were shown in G. (H) 1×10^6 *circGTIC1* overexpressing and control cells were injected into BALB/c nude mice, and tumor volumes were measured every three days. (I) Tumor invasion assay was performed using *circGTIC1* overexpressing and control cells. 36 hours later, typical images were collected and invaded cells were counted. Scale bars,

50 μm. (J) circGTIC1 highly expressed and lowly expressed samples were collected and the indicated proteins were examined. β-actin served as a loading control. (K, L) circGTIC1 highly expressed and lowly expressed samples were collected for sphere formation assay (K) and transwell invasion assay (L). (M) circGtic1 overexpressing mice were generated by hydrodynamic injection, and gastric tumors were induced by MNNG/ helicobacter pylori. Six months later, tumor numbers and tumor volumes were shown. Eight mice were used per group.

Figure 4. circGTIC1 drove Sox8 expression. (A) *circGTIC1* knockout cells and control cells were used for transcriptome analysis, and differently expressed genes were shown. Sox8 was the lowest expressed transcription factor in *circGTIC1* knockout cells. (B, C) Sox8 expression levels in *circGTIC1* knockout cells (B) and circGIC1 overexpressing cells (C) were examined by Western blot. β-actin was a loading control. (D) Sox8 expression levels in gastric tumor were examined by realtime PCR and showed positive co-correlation with circGTIC1 expression. (E) RNA was extracted from circGTIC1 highly-expressed and lowly-expressed samples, followed by Sox8 examination with Northern blot. 18S rRNA was a loading control. (F) *Sox8* knockout cells were generated through CRISPR/Cas9 approach, and knockout efficiency was confirmed by Western blot. (G, H) circGTIC1 was silenced in *Sox8* knockout cells, followed by sphere formation (G) and transwell invasion (H) assay. Typical images and ratios were shown. (I, J) *Sox8* knockout cells were used for circGTIC1 overexpression, and then used for sphere formation assay (I) or transwell assay (J).

Figure 5. circGTIC1 interacted with Ino80 complex. (A) circGTIC1 probes targeting the conjunction sequence of circGTIC1 were used to identify the interaction protein of circGTIC1. Ino80 was identified to combine with circGTIC1. (B) The combination between circGTIC1 and Ino80 complex was confirmed by Western blot. (C) Ino80 RIP assay was performed, and the enrichment of circGTIC1 was examined by realtime PCR. IgG was an antibody control. (D) The direct combination of Ino80 and circGTIC1 was detected by electrophoretic mobility shift assay (EMSA). Ino80 antibody was also used for super-shift. (E) The co-localization of circGTIC1 and

Ino80 was examined by double FISH, and counterstained with DAPI. (F) The expression levels of Ino80 components were examined by realtime PCR. (G) TICs, spheres and invaded cells were collected to detect the expression of Ino80 complex. Three components of Ino80 complex were examined. (H) Non-spheres (N) and spheres (S) derived from primary samples were used for Ino80 complex detection. β -actin was a loading control.

Figure 6. circGTIC1 recruited Ino80 complex to Sox8 promoter. (A, B) Ino80 ChIP assay (A) and circGTIC1 ChIP assay (B) were performed, and the enrichment of the indicated regions of *Sox8* promoter was examined by realtime PCR. (C, D) ChIP assay of Ino80 complex was performed using *circGTIC1* knockout cells (C) or overexpressing cells (D), and the enrichment of *Sox8* promoter was examined by realtime PCR. (E) *circGTIC1* knockout and control TICs were used for *Sox8* promoter detection. Impaired co-localization of *Sox8* promoter and Ino80 complex was observed upon *circGTIC1* knockout. (F) Ino80 ChIP eluate samples were used for size fractionation with sucrose gradient ultracentrifugation. For Ino80 component examination, the fractions were subjected into SDS-PAGE and detected by the indicated antibodies. For *Sox8* promoter examination, DNA was extracted from fractions, followed by PCR. *circGTIC1* knockout and control cells were used for Ino80 ChIP assay. (G) *Ino80* knockout cells were generated and impaired *Sox8* expression was observed. (H, I) *circGTIC1* or *Ino80* knockout inhibited the activation of *Sox8* promoter, and circGTIC1 overexpression drove an opposite role. (J, K) *circGTIC1/Ino80* knockout (J) and circGTIC1 overexpression (K) cells were used for H3K4me3 detection. The enrichment of H3K4me3 in *Sox8* promoter was examined by realtime PCR. (L, M) RNA polymerase II enrichment in *Sox8* promoter was detected by ChIP assay. *circGTIC1/Ino80* knockout cells (L) and overexpressing cells (M) were used for ChIP assay. (N) circGTIC1 was overexpressed in *Ino80* knockout or *Sox8* promoter knockout cells, and then *Sox8* expression was detected by Western blot. (O, P) circGTIC1 was overexpressed in *Ino80* knockout cells and *Sox8* promoter knockout cells, followed by sphere formation assay (O) or transwell invasion assay (P).

Figure 7. Sox8 played an essential role in gastric TICs. (A) Sox8 expression in peri-tumor, early gastric and advanced gastric samples was detected by realtime PCR. (B) Six pairs of gastric tumors (T) and non-tumors (N) were used for Sox8 detection with Western blot. β -actin was a loading control. (C) Sox8 expression profiles in the indicated samples were examined by IHC. Typical images were shown. Scale bars, 50 μ m. (D) Gastric tumor patients were divided into two groups according to *circGTIC1* expression, followed by Kaplan-Meier survival analysis. (E) Spheres (S) and non-spheres (N) derived from the indicated samples were used for Sox8 detection. β -actin was a loading control. (F) TICs were detected in *Sox8* knockout samples with FACS, and TIC ratios were shown as mean \pm s.d. (G) *Sox8* knockout cells were used for sphere formation assay. Typical images and sphere-initiating ratios were shown. (H) The ratios of proliferate cells upon *Sox8* knockout were examined by Ki67 staining. (I) *Sox8* knockout cells were used for transwell invasion assay. Typical images and invasive cell numbers were shown. (J) *Sox8* was rescued in *circGTIC1* knockout cells. *Sox8* expression levels were examined by Western blot. (K, L) *Sox8* rescued *circGTIC1* knockout cells were used for sphere formation assay (K) and transwell invasion assay (L). Typical images were shown in left panels and ratios were shown in right panels.

Figure 1

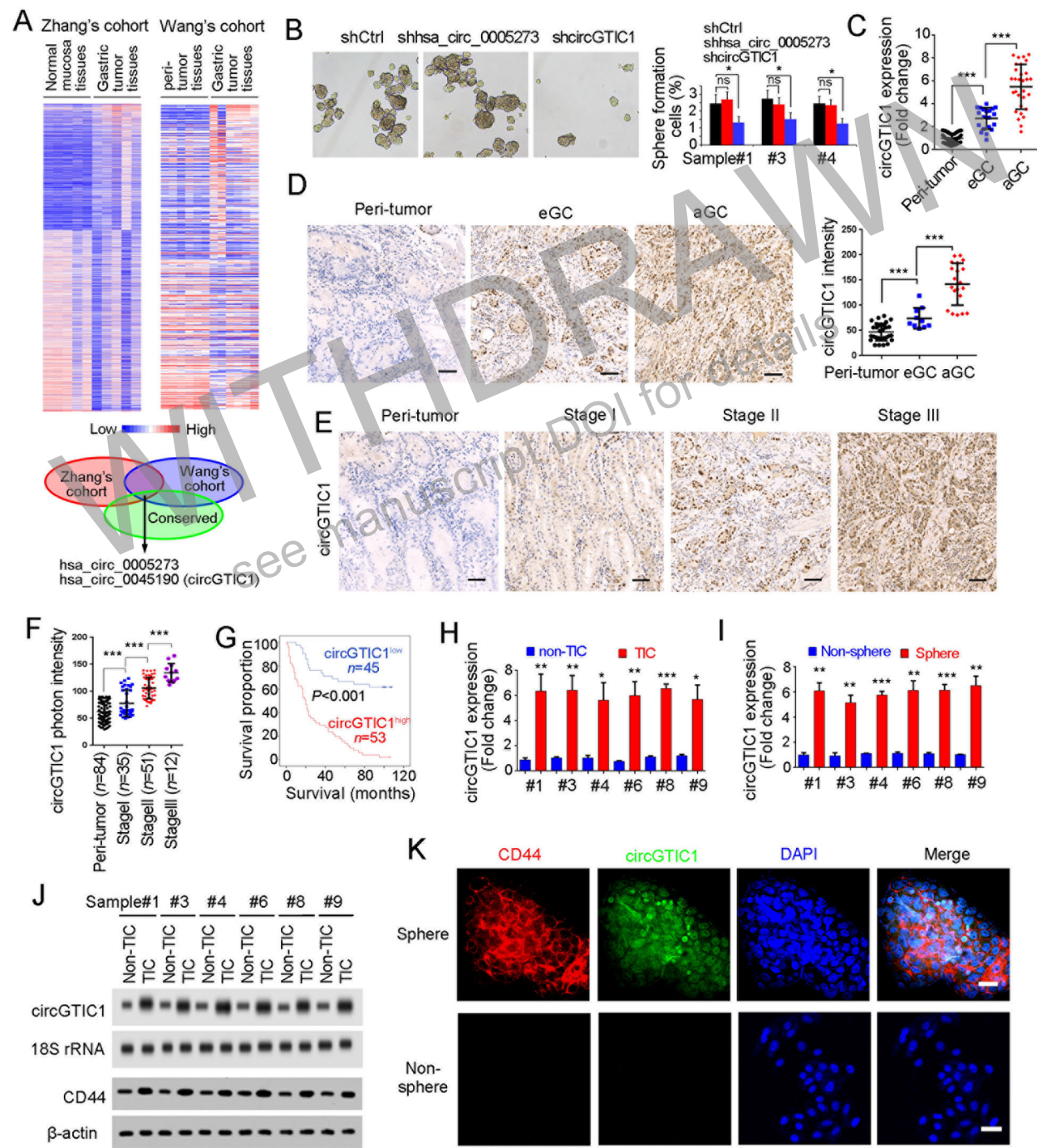


Figure 2

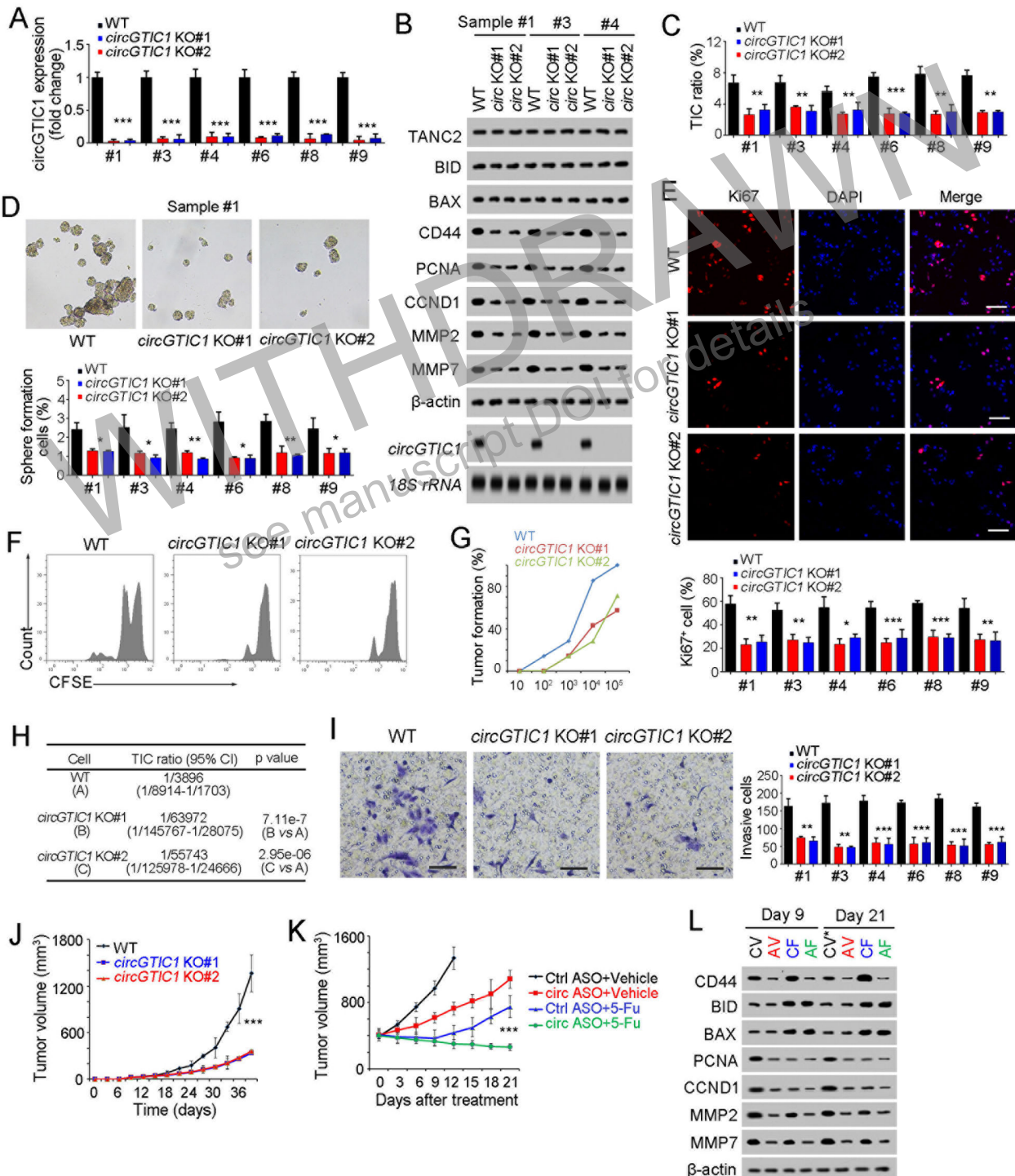


Figure 3

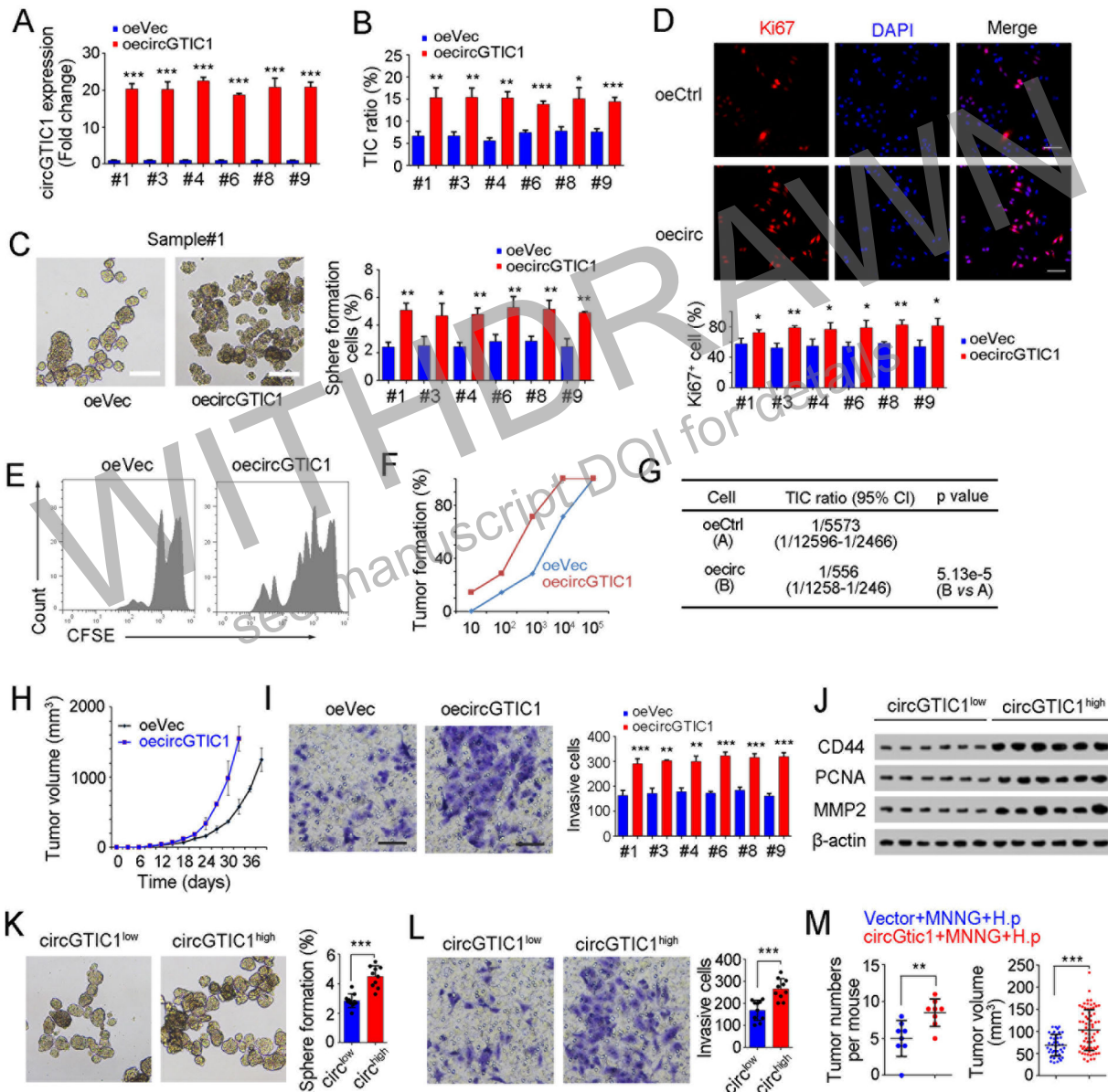


Figure 4

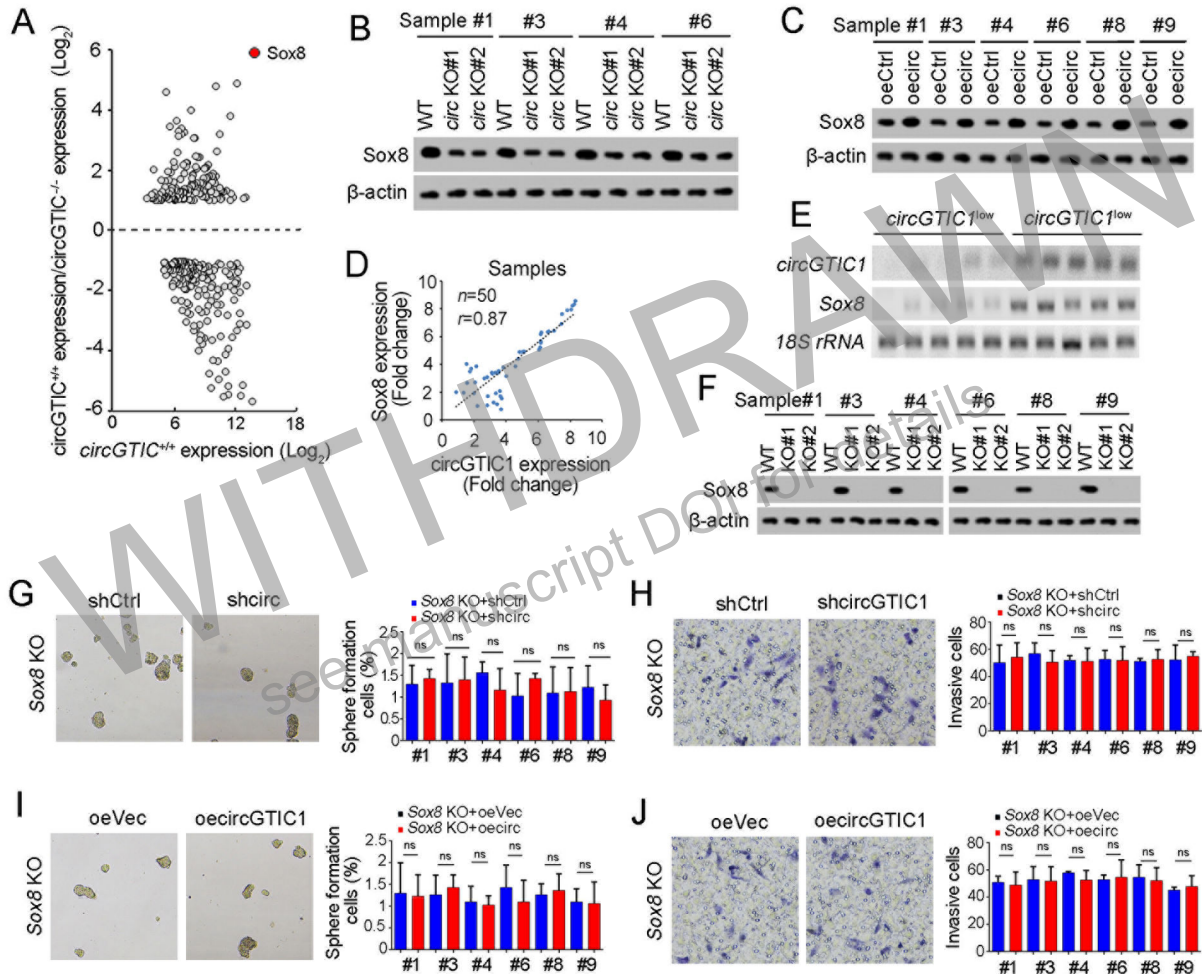


Figure 5

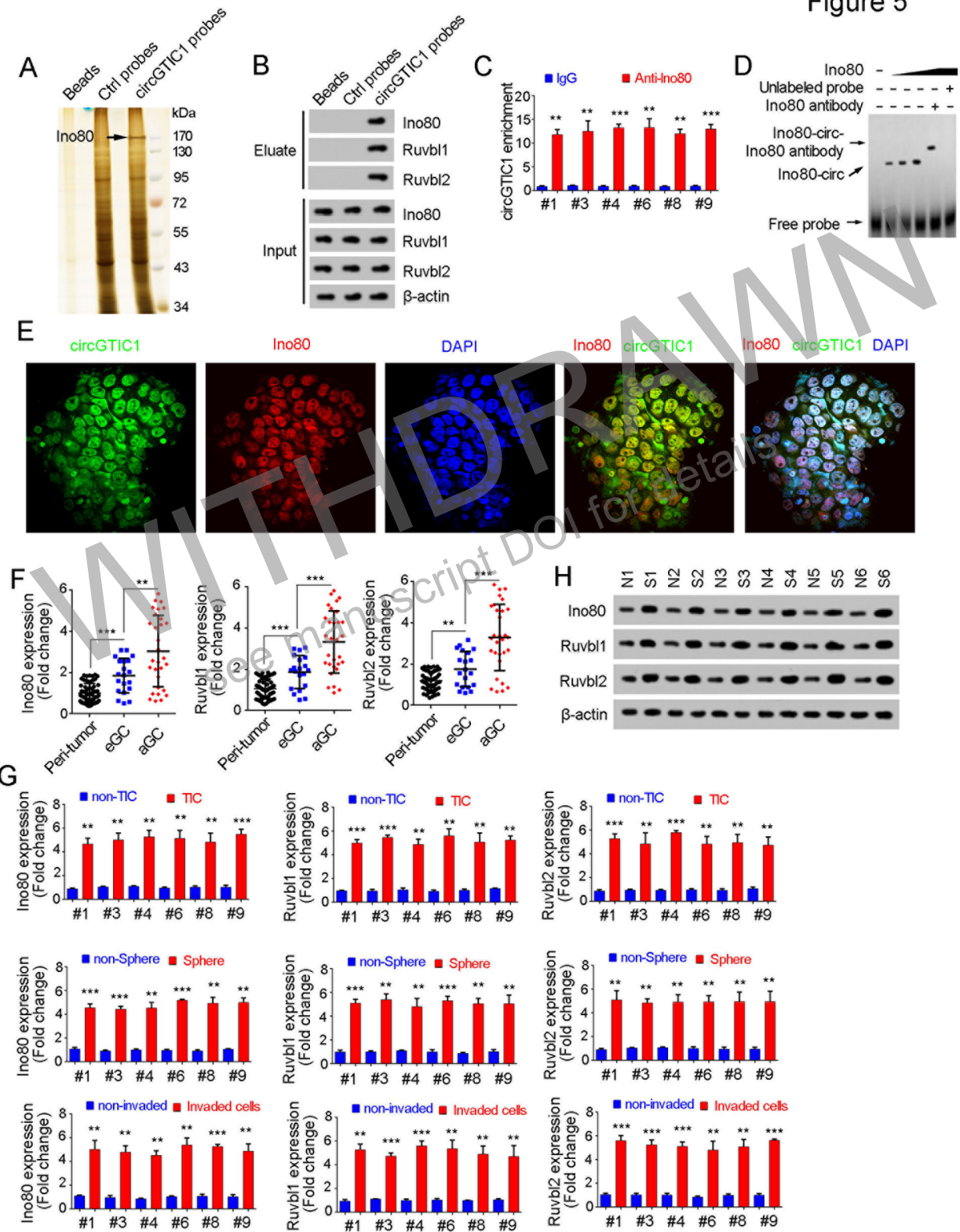


Figure 6

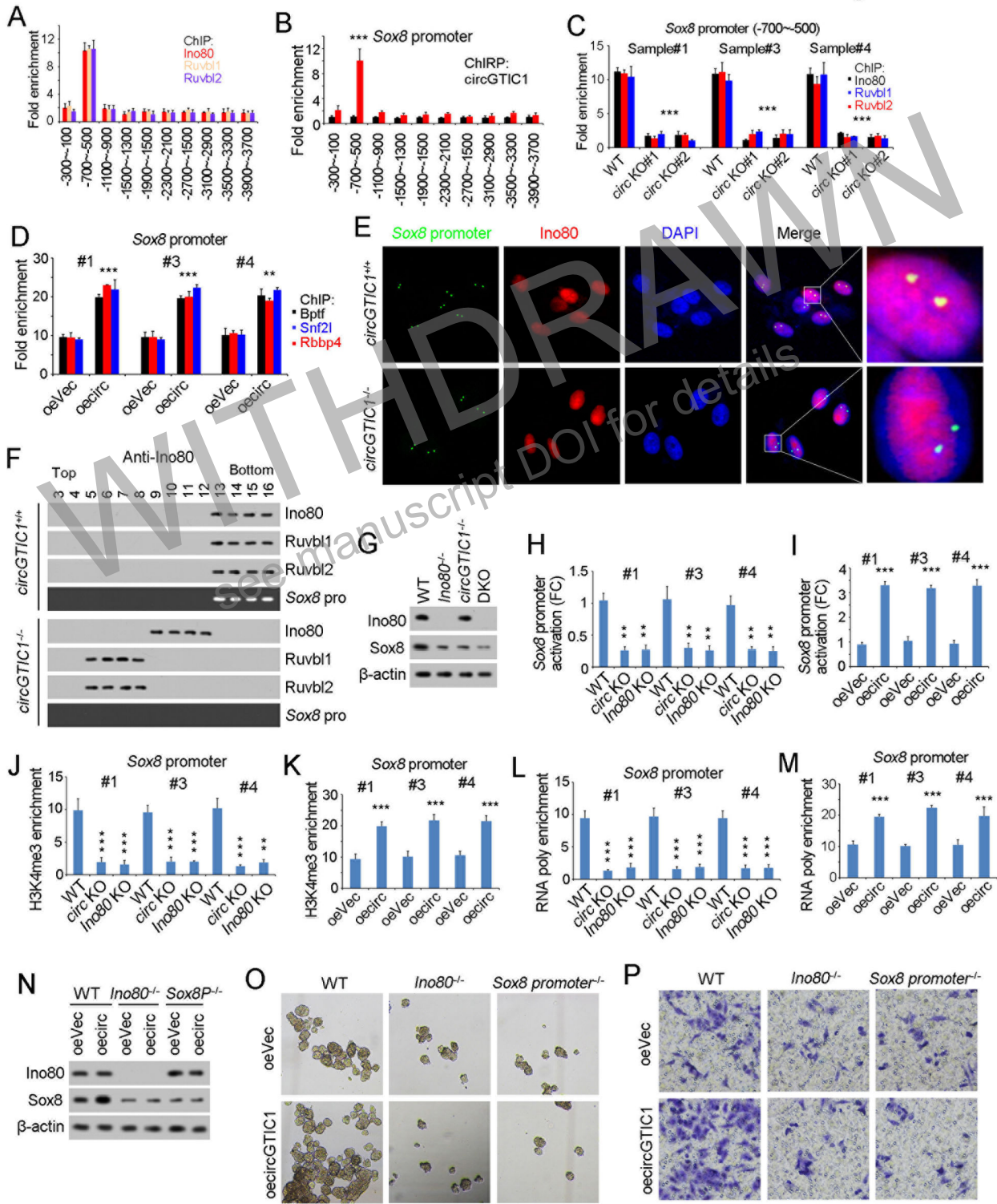


Figure 7

